

# Design and Simulation of Mushroom Nanorods for Plasmonic Applications Using FDTD Methods and Deep Learning

Tanjoy Mahmud<sup>1\*</sup>, Aminul Islam<sup>2</sup>, Atia Farzana Chowdury<sup>3</sup>, Md Maruf Hossain<sup>4</sup>

<sup>1,4</sup>School of Electronics and Information Engineering, Nanjing University of Information Science & Technology, Nanjing, China.

<sup>2,3</sup> College of Computer Science, Nanjing University of Aeronautics and Astronautics, Nanjing, China

\*Corresponding Author: mahmudtanjoy@nuist.edu.cn

\*\*\*\*\*

## Abstract:

This paper introduces a dataset generated through Finite-Difference Time-Domain (FDTD) simulations, focusing on the electromagnetic behavior of Mushroom Nanorods. The dataset captures a range of numerical parameters and field images across different configurations, including materials like Gold, Al<sub>2</sub>O<sub>3</sub>, and SiO<sub>2</sub>. These simulations are intended to advance research in photonics, optics, and electromagnetic wave dynamics. The dataset also serves as a key resource for machine learning models, specifically reinforcement learning, aimed at improving the prediction accuracy of electromagnetic field behavior influenced by material properties and structural variations. In comparison to other existing datasets in the field, our dataset offers a more comprehensive and parameterized set of images and simulation data, which allows for a deeper understanding of field behavior in nanophotonic systems. This work not only contributes to the development of more efficient photonic devices but also highlights the potential of using simulation-driven data for optimizing nanostructure designs in various research areas, including nanophotonics and electromagnetic modelling.

*Keywords* — Mushroom nanorods, numerical FDTD, deep learning, photonics and plasmonics simulation, Electromagnetic field distribution.

\*\*\*\*\*

## I. INTRODUCTION

The continuous advancement of photonics, nanotechnology, and material sciences heavily relies on the ability to model light and electromagnetic fields accurately within various mediums. As these fields progress, the need for sophisticated simulation techniques that can effectively handle the complexity of nanostructures and their interaction with light has become more pressing. Among the various simulation methods available, the Finite-Difference Time-Domain (FDTD) technique stands out as one of the most accurate and widely adopted approaches for solving Maxwell's equations in the time domain. FDTD allows researchers to study the interaction of electromagnetic waves with materials at the nanoscale, providing crucial insights into the

behavior of light in complex nanostructured environments [1]. Given the vast potential of FDTD simulations in modeling electromagnetic field distributions, simulation datasets have become increasingly important for advancing research in photonics and nanophotonics. These datasets, which capture electromagnetic field data under various material and geometric configurations, offer reusable information that can significantly reduce the need for extensive experimental setups. Such datasets are essential not only for experimental researchers looking to test their theories but also for machine learning communities that aim to develop predictive models based on these simulations. The integration of machine learning with simulation data, particularly deep learning models, has shown

promise in accelerating the design and optimization processes for photonic devices [2].

However, a significant limitation of many commonly available simulation datasets is their lack of a comprehensive range of parameters. Often, these datasets focus on narrow material types or geometries, limiting their applicability across a broad spectrum of real-world applications. This paper addresses this gap by presenting a new and expansive dataset generated through FDTD simulations of Mushroom Nanorods, a type of nanostructure that is gaining considerable interest due to its unique optical properties. The dataset includes various material configurations, such as Gold, Al<sub>2</sub>O<sub>3</sub>, and SiO<sub>2</sub>, and provides detailed electric field maps recorded as images for a wide array of geometric and material parameters. These data are critical for understanding the electromagnetic response of these nanostructures under different conditions, from plasmonic interactions to light trapping.

The dataset introduced in this paper serves a dual purpose. First, it offers valuable resources for optical and photonics engineers who need high-fidelity simulations to guide their advanced designs and experimental setups. Second, it acts as a training set for deep learning models, which can predict electromagnetic behavior based on input material properties, device structure, and geometric configurations. The use of deep learning in combination with FDTD simulations has the potential to revolutionize the way photonic devices are designed, making the process more efficient, accurate, flexible, and scalable [3]. By providing a comprehensive, parameterized dataset that includes diverse material types, shapes, and geometries, this research contributes to both experimental and machine learning communities, enabling further advancements in the rapidly evolving field of nanophotonics.

## **II. RELATED WORK**

Several studies have focused on developing datasets derived from FDTD simulations to predict and enhance the performance of photonic structures. Krasikov, Tranter, and Bogdanov (2022) explored the application of machine learning in metaphotonics, emphasizing the need for larger datasets to improve

the precision and efficiency of photonic devices. Their work highlights the importance of acquiring extensive simulation data to refine models and enhance device performance, thus demonstrating the synergy between FDTD simulations and AI-driven optimization methods [4].

Similarly, Kuhn et al. (2023) demonstrated how FDTD-derived datasets can be utilized with graph neural networks to predict electromagnetic field responses in photonic devices. This work provides strong evidence that machine learning models, particularly graph neural networks, can successfully predict the behavior of electromagnetic fields based on FDTD simulations, offering an efficient method to optimize photonic systems without exhaustive physical testing [5].

Ali et al. (2023) further extended the use of machine learning by applying FDTD simulations to predict strongly localized resonant modes of light in disordered arrays of dielectric scatterers. They addressed the challenges posed by the electromagnetic field interactions within these arrays and showed how machine learning could refine FDTD simulation results to predict light behavior in complex materials more accurately. This work demonstrates the potential for machine learning models to extract useful insights from FDTD simulations for photonic design [6].

In a similar vein, Ma et al. (2021) leveraged neural networks to optimize the design of advanced photonic structures. They utilized a dataset containing FDTD-simulated electromagnetic fields to train models that could improve photonic architecture design. Their research underscores the growing potential of deep learning in modern photonics, using FDTD datasets to streamline the development of photonic devices with enhanced performance and functional characteristics [7].

Moreover, Zhelyuzhenkov (2019) and Brunton & Majumdar (2011) explored the use of deep learning to accelerate the scatterer-to-field mapping in dielectric metasurfaces, demonstrating the importance of large datasets derived from FDTD simulations for fast, iterative design optimization. Their work illustrates how deep learning models can be employed for the inverse design of metasurfaces,

which has significant implications for the design of next-generation photonic devices [8].

Kanmaz et al. (2023) focused on generating FDTD datasets for near-field electromagnetic identification and reverse design of metasurfaces. By combining these datasets with deep learning, they showed how machine learning could determine optimal metasurface geometries and parameters to meet specific target field distributions. This approach represents a novel use of FDTD simulations in conjunction with deep learning for practical applications in metasurface design [9].

Liu et al. (2021) also highlighted the role of machine learning in photonic inverse design. Their work showed how a dataset of FDTD-simulated electromagnetic fields could be used to train models for the inverse design of photonic systems. This method reduced design time and improved the efficiency of photonic device development by enabling faster exploration of design possibilities through machine learning [10].

Singh et al. (2020) employed FDTD simulations to design light meta-structures in integrated photonics, with a particular focus on beam design. Their use of deep learning algorithms to design customized beam profiles further demonstrates the potential of FDTD-based datasets for designing optical components tailored to specific applications [11].

In the same vein, Li et al. (2020) utilized deep neural networks (DNN) to predict electromagnetic scattering from complex nanostructures using carefully prepared FDTD datasets. Their study showed that DNN models trained on these datasets could accurately predict scattering behavior with a high degree of accuracy, while significantly reducing computational time and resource consumption compared to traditional FDTD simulations [12].

Finally, Malkiel et al. (2017) presented an efficient method for classifying and retrieving nanophotonic structures using deep learning. Their work utilized FDTD simulation data to train models for the design and retrieval of nanophotonic structures, further emphasizing the role of simulation-based datasets in accelerating the development of nanophotonic devices [13].

### III. METHODOLOGY

This section outlines the method used to create the dataset, focusing on the FDTD simulation process and the parameters adjusted during each run [14]. The simulations conducted using FDTD Solutions software, model electromagnetic wave behavior in structures made of Gold, Aluminum Oxide ( $\text{Al}_2\text{O}_3$ ), and Silicon Dioxide ( $\text{SiO}_2$ ). The structure is divided into three parts: the light source,  $\text{Al}_2\text{O}_3$  and  $\text{SiO}_2$  layers, and the Au mushroom Nanorod layer. A 2D and 3D design was used, with grey light as the source. Outputs were captured by T and R monitors at the bottom and top of the structure, respectively. The mushroom shape was created using a circle and sphere with a 50 nm radius. Throughout the simulation runs, various parameters were adjusted, including different geometries of the structures, material layers, source positions, and boundary conditions to observe the effects on the electromagnetic fields.

#### A. Description of the Used Material:

##### Gold (Au)

**Type:** Metal

**Electromagnetic Properties:** Gold is highly reflective and exhibits strong plasmonic characteristics due to its negative permittivity in the visible and near-infrared frequencies. This makes it an ideal material for plasmonic devices, sensors, and waveguides.

**Simulation:** For simulations, gold is modeled using the Drude-Lorentz model or data from material databases like the Palik database. The software records the frequency-dependent permittivity of gold, as its optical behavior varies across frequencies. FDTD simulations can also model Surface Plasmon Polaritons (SPPs), electromagnetic waves that travel along gold's surface.

##### Aluminum Oxide ( $\text{Al}_2\text{O}_3$ )

**Type:** Dielectric

**Electromagnetic Properties:**  $\text{Al}_2\text{O}_3$  is a transparent, colorless dielectric material with a relatively high refractive index (r.i.  $\approx 1.77$  in the visible range). It is widely used in optical and photonic applications.

**Simulation:** In the simulation,  $\text{Al}_2\text{O}_3$  is modeled as a non-dissipative medium, simplifying its computational modeling. Its higher refractive index makes it suitable for use in multilayered photonic structures and optical waveguides.  $\text{Al}_2\text{O}_3$  is also used

in cladding structures to control light propagation in photonic devices.

### **Silicon Dioxide (SiO<sub>2</sub>)**

**Type:** Dielectric (amorphous)

**Electromagnetic Properties:** SiO<sub>2</sub> is a transparent dielectric with a refractive index of about 1.45 in the visible range. It is commonly used in optical fibers, waveguides, and lenses.

**Simulation:** In FDTD simulations, SiO<sub>2</sub> is modeled as a lossless dielectric. It serves as a substrate or cladding material in waveguides, with its refractive index adjustable using dispersion models like the Sellmeier equation.

### **B. Example Use Cases for These Materials in Simulations:**

**Plasmonic Devices:** Gold nanoparticles or thin films, surrounded by Al<sub>2</sub>O<sub>3</sub> or SiO<sub>2</sub>, support surface plasmons. This simulation improves light-matter coupling at the nanoscale, which is useful for sensing or enhancing fields in near-field optics.

**Anti-Reflection Coatings:** SiO<sub>2</sub> is commonly used in coatings to minimize reflection through destructive interference. Thin films of SiO<sub>2</sub> on gold substrates can be modeled to reduce reflection.

**Optical Waveguides:** SiO<sub>2</sub> and Al<sub>2</sub>O<sub>3</sub> are used in waveguide structures, where light is confined in a high refractive index medium (Al<sub>2</sub>O<sub>3</sub>) and surrounded by a lower refractive index medium (SiO<sub>2</sub>) for effective light guidance. FDTD simulations help accurately model light paths with minimal reflection, low propagation loss, and strong confinement, making them essential for optimizing integrated photonic circuit designs.

### **C. Practical Considerations in FDTD Solutions:**

**Meshing:** To capture plasmonic effects near the surface of gold, a fine mesh is used around the gold structures to account for significant field variations in the simulation.

**Material Dispersion:** Both Al<sub>2</sub>O<sub>3</sub> and SiO<sub>2</sub> exhibit dispersion, where the refractive index changes with wavelength. It is important to choose the correct dispersion model in FDTD to accurately represent these materials in the simulation.

**Boundary Conditions:** For structures involving these materials, Perfectly Matched Layers (PML) are used

to minimize reflections at the edges of the simulation domain.

The following parameters were systematically varied in the simulation (detailed in the CSV file):

- **Image Path:** Specifies the folder where images from the simulation are saved.
- **Circle\_x\_min, Circle\_x\_max, Circle\_radius:** Define the x-axis range and the radius of the circular area representing material or source regions.
- **Boundary\_layer\_min, Boundary\_layer\_max:** Set the thickness and profile of the boundary layers through which electromagnetic waves pass, affecting reflection or absorption.
- **Source\_x\_min, Source\_x\_max, Source\_y\_min, Source\_y\_max:** Define the area of the light source that emits electromagnetic waves.
- **Monitor\_x\_min, Monitor\_x\_max, Monitor\_y\_min, Monitor\_y\_max:** Specify monitor locations to measure electromagnetic fields at different points during the simulation.
- **Mesh\_x\_min, Mesh\_x\_max, Mesh\_y\_min, Mesh\_y\_max:** Control the limits in the x and y directions for discretizing the simulation space. Higher mesh density results in more detailed geometry but also increases computational load.
- **Gold\_x\_min, Gold\_x\_max, Gold\_y\_min, Gold\_y\_max, Gold\_z\_min, Gold\_z\_max:** Define the position and thickness of the gold layer, which is important for plasmonic effects significantly influencing the local field strength distribution.
- **Al<sub>2</sub>O<sub>3</sub>\_x\_min, Al<sub>2</sub>O<sub>3</sub>\_x\_max, Al<sub>2</sub>O<sub>3</sub>\_y\_min, Al<sub>2</sub>O<sub>3</sub>\_y\_max, Al<sub>2</sub>O<sub>3</sub>\_z\_min, Al<sub>2</sub>O<sub>3</sub>\_z\_max:** Specify the location and dimensions of the Al<sub>2</sub>O<sub>3</sub> layer in the simulation.
- **SiO<sub>2</sub>\_x\_min, SiO<sub>2</sub>\_x\_max, SiO<sub>2</sub>\_y\_min, SiO<sub>2</sub>\_y\_max, SiO<sub>2</sub>\_z\_min, SiO<sub>2</sub>\_z\_max:** Define the size and position of the SiO<sub>2</sub> layer, used as a dielectric material in the simulation.
- **Source\_z\_min, Source\_z\_max:** Set the z-axis limits of the source's position, controlling the emission of electromagnetic waves along the z-axis.

- Monitor\_z\_min, Monitor\_z\_max: Specify monitoring planes in the z-direction for capturing electromagnetic field data.
- Mesh\_z\_min, Mesh\_z\_max: Control discretization in the z-direction, contributing to the simulation's spatial resolution.
- Monitor\_point: Designates the location where electromagnetic fields are observed during the simulation.
- Mesh\_step: Controls the spacing between nodes, which determines the level of detail in the simulation.

For each parameter set, 10 images were generated per simulation run, leading to a total of 100 images. These images clearly show the electromagnetic field distribution and the material interactions during the simulation, providing useful insights into how waves propagate through and around different nanostructures under various conditions. They are essential for validating simulation accuracy and understanding the performance of designed models.

**e.** The dashed and solid lines represent the electric field (E-field) configuration within the simulation. These images illustrate the magnitude and direction of the electric field vectors at different locations in the simulation space, helping researchers identify areas of strong field enhancement, interference patterns, and field decay. This detailed visual information supports the analysis of plasmonic behavior, resonance effects, and energy confinement in complex photonic structures.

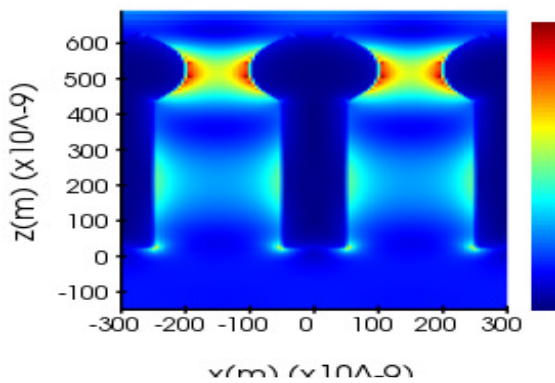


Fig. 1 e field

**e1:** A specific alteration or a particular component of the electric field (e.g., the E-field along a certain direction).

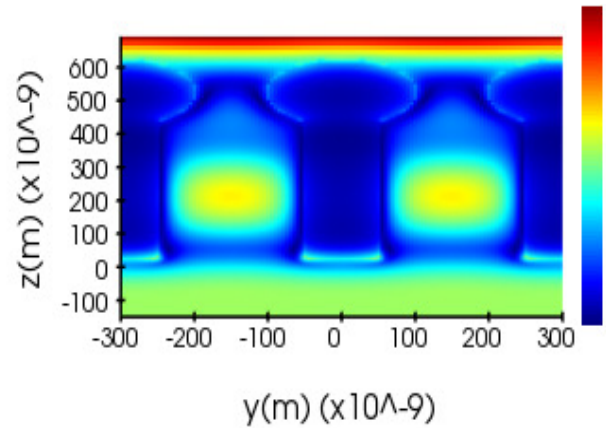


Fig. 2 e field in a certain direction

**field:** Refers to the complete electromagnetic field, which includes both the electric and magnetic components.

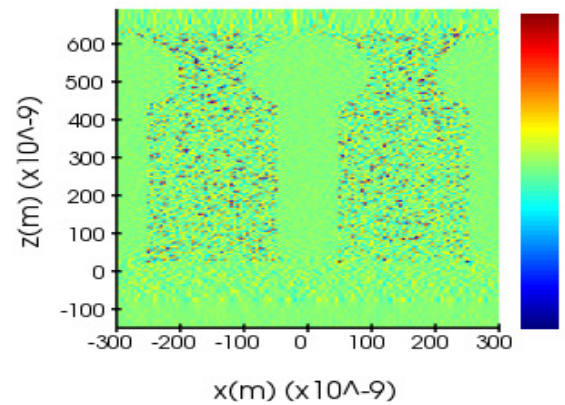


Fig. 3 field

**h1:** Represents the magnetic field (H-field), utilized to examine the behavior of magnetic field components within the simulation domain.

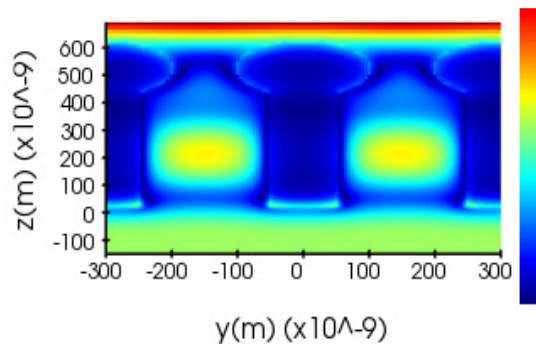


Fig. 4 h field

**p:** P-field or energy field indicating the strength or distribution of power over the simulation domain.

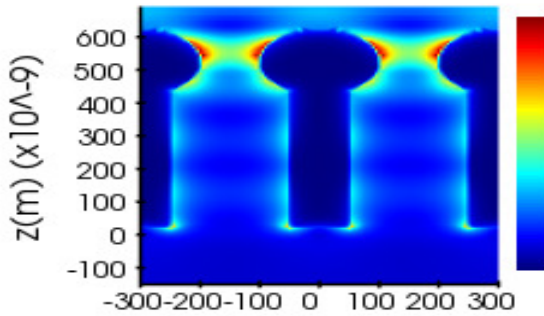


Fig. 5 P field or energy field

**p1:** A subset of power density, specifically developed to focus on certain directions or field quantities.

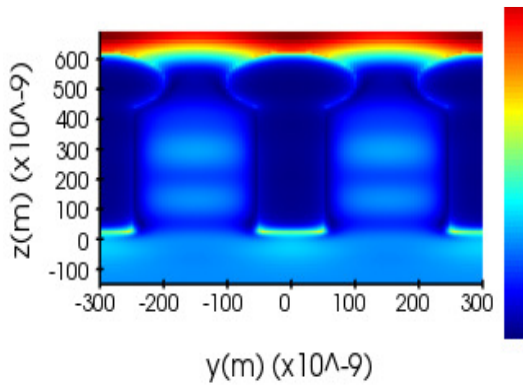


Fig. 6 P-field or Energy Distribution in a Specific Direction

**Spectrum:** These images show the spectral response, including transmission and reflection of electromagnetic waves through the materials.

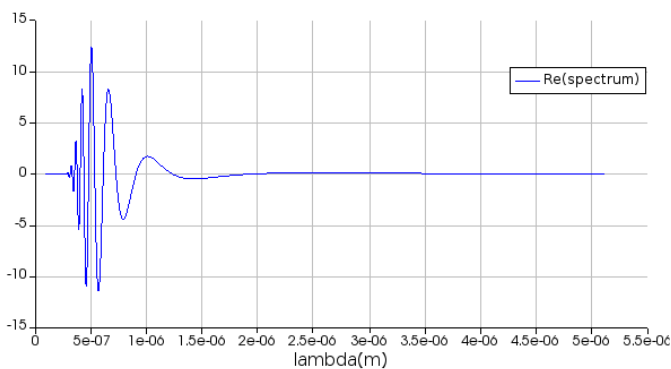


Fig. 7 Spectrum response

**t:** Explains how the electromagnetic fields of the simulation change in the progress of time during the evaluation of the fields.

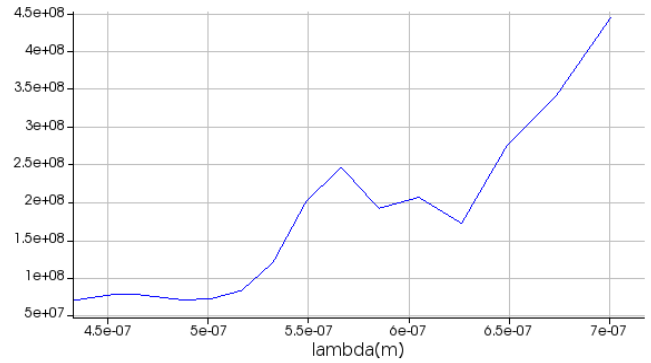


Fig. 8 Time progress during the evaluation

**t1:** Some variation of the domain results in the time domain, which provides information about one aspect of the field behavior over time.

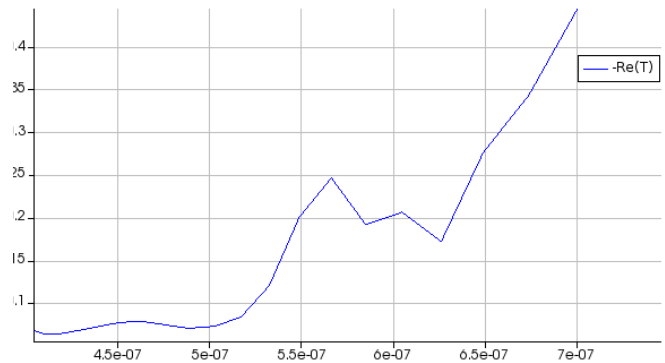


Fig. 9 A Temporal view of field behavior

**Time:** Captures the overall temporal evolution of the electromagnetic fields, reflecting their time-varying nature across the entire system.

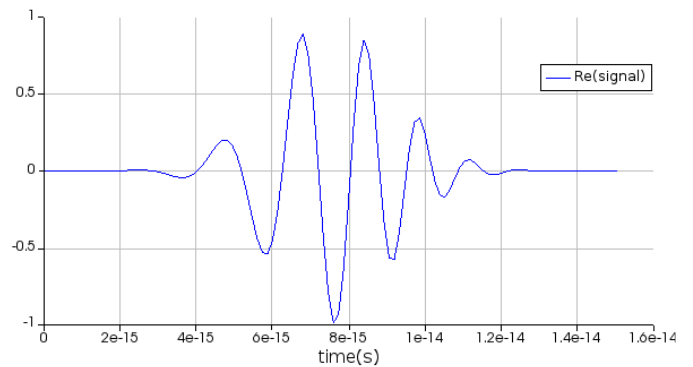


Fig. 10 Time-dependent behavior of the fields

#### D. Simulation, Workflow, and Data Generation

The dataset was generated through multiple simulation runs, each with varying parameter values. Gold,  $\text{Al}_2\text{O}_3$ , and  $\text{SiO}_2$  were used as materials, with the source configurations and system geometry entered the FDTD software to generate electromagnetic fields. Observations of the fields were made at various points within the simulation domain. The resulting data, including electric fields, magnetic fields, and power distribution, were stored as images. A corresponding CSV file was created to link each parameter to its respective ImageSet.

#### E. Dataset Composition and Parameter Descriptions

The dataset is structured with multiple rows in a CSV file, each corresponding to a specific simulation setup and its defined parameter configuration. Each row includes the Image Path column, which points to the directory containing the images generated for that particular simulation case. Variable columns such as Circle\_x\_min, Gold\_x\_min, and Source\_z\_min provide the spatial and material details of the simulation for each field image. The images are further categorized by type (e, e1, field, etc.) to visualize the electromagnetic properties at different time steps or field components. This organized approach ensures that each row contains all relevant parameter values, metadata, and their associated field image.

#### F. Simulation Structure

The 2D top view of the simulation domain displays the distribution of electric and magnetic fields in the x-y plane. The image shows the strength of these fields across a cross-sectional slice of the simulation space. The grey squares and the grid lines indicate the discretization used in the FDTD method, where each square represents a point where the solution to Maxwell's equations is calculated. The central circular area (colored blue or cyan) may represent a nanoparticle, a dielectric material such as  $\text{Al}_2\text{O}_3$  or  $\text{SiO}_2$ , or a region with differing field properties compared to the surrounding areas. The color map reflects field intensity, with color changes corresponding to variations in field strength. Blue and cyan areas indicate regions of low field intensity,

while magenta or pink regions represent areas with higher field intensity or boundary effects.

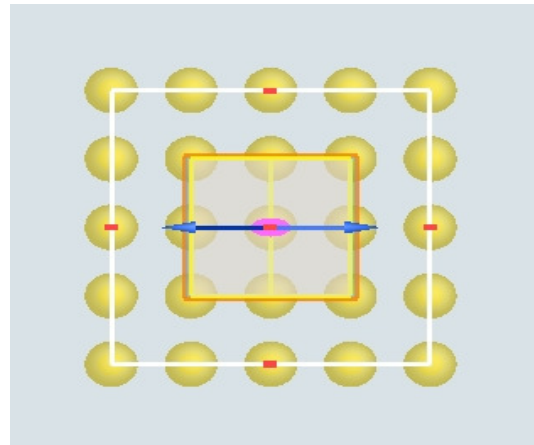


Fig. 11 2D perspective view of the simulation domain

Before evaluating the results, it's important to consider the 3D perspective of the simulation domain. This view provides insight into the simulation geometry, material layers, sources, and boundary conditions. The box-shaped structure represents the simulation domain, surrounded by PML or ABC to prevent boundary reflections. The purple and orange boxes represent different material layers, such as metallic layers (Gold) or dielectric regions ( $\text{Al}_2\text{O}_3$ ,  $\text{SiO}_2$ ). A transparent horizontal plane in the middle shows the monitoring plane where field data, like field intensity at a specific height, are recorded. This image helps visualize the placement of materials, field sources, and boundaries, which are crucial for analyzing electromagnetic wave interactions. The left elevated view shows the simulation domain with the field source in place.

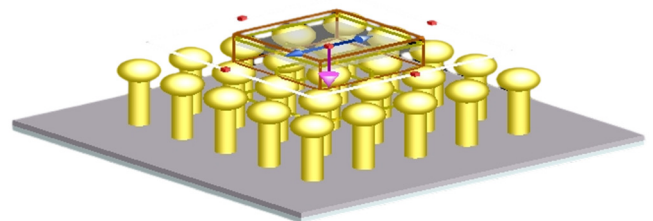


Fig. 12 3D simulation view

This side view shows the internal structure of the simulation domain in 2D. The white and yellow areas represent materials like Gold,  $\text{Al}_2\text{O}_3$ , and  $\text{SiO}_2$ .

Arrows indicate the wave propagation direction or current generated by the source, typically placed at the center or boundary. The grey grid represents the FDTD mesh, with smaller cells near material interfaces for more detail and larger cells in less detailed areas.

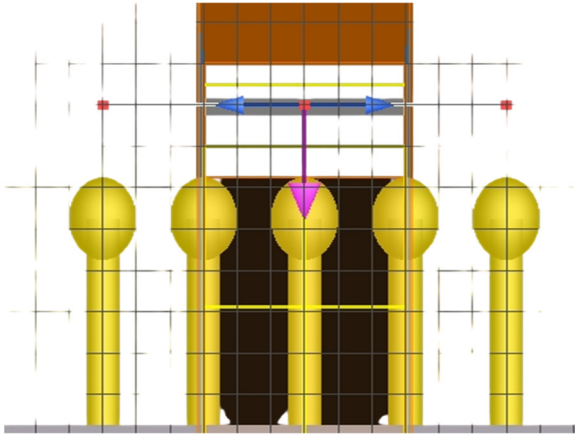


Fig. 13 2D inner simulation zone

This vertical cross-section shows the simulation domain from another angle, with key parts labelled. The field source is represented in purple, and a monitoring point is shown in blue. The arrow from the source (purple region at the bottom) indicates the initial field direction or source location. The blue sphere and dashed line represent the monitoring point where field quantities, like electric or magnetic field strength, are measured.

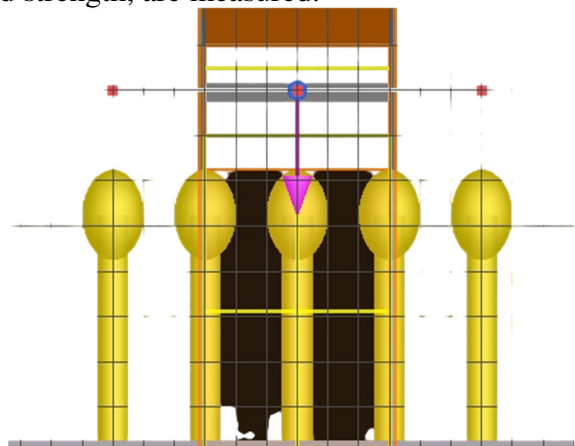


Fig. 14 Vertical Cross-Section with Field Source and Monitors

The vertical orange lines indicate regions of localized field interaction or boundary conditions that prevent reflection interference at the domain's edges.

**G. Impact of The Dataset on Advancing the Research Field**  
**Data-Driven Simulation Analysis:** The dataset helps researchers understand the impact of various parameters on electromagnetic field characteristics. It provides both raw data and simulation images, revealing trends between parameters and outcomes.

**Machine Learning Applications:** The dataset can be used to train predictive models, improving the simulation and optimization of photonic devices, antennas, and sensors.

**Optimization Studies:** Researchers can use the data to optimize design parameters, such as boundary layers and source positions, for AI-driven photonic and optical designs.

**Valuable for Experimentalists:** The dataset offers a practical guide for experimental researchers, helping refine setups by comparing simulation results to real-world data.

**Studying Electromagnetic Phenomena:** Our simulation data is crucial for studying light-matter interactions in fields like plasmonic and nano-optics, greatly aiding the efficient design of devices like waveguides, photonic crystals, and advanced optical sensors.

**H. Uses and Application of The Dataset**

**Photonics and Nanotechnology:** This dataset is crucial for research on light interaction with nanostructured surfaces. Researchers in plasmonics and metamaterials can use it to optimize device designs, such as improving light absorption in solar cells or enhancing signal transmission in optical waveguides.

**Deep Learning:** The dataset is well-suited for deep learning applications, including electronics design and model training. Potential uses include:

- **Field Prediction Models:** Training models to predict electromagnetic field distribution based on given parameters, allowing for faster design iterations.
- **Inverse Design:** Using deep learning to determine the optimal material configurations and geometries for specific field behaviors, improving fabrication efficiency.

#### IV. CONCLUSION

This dataset provides a comprehensive and flexible resource for researchers in photonics, electromagnetics, and deep learning. With its wide range of parameters and corresponding electromagnetic field distribution images, it enables optimization studies, accelerates design processes, and opens new possibilities for machine learning in optical simulations. Its broad applicability ensures it will play a key role in advancing academic research and industrial development, particularly in AI-driven workflows for nanophotonic sensor design and optimization.

#### ACKNOWLEDGMENT

I would like to express my sincere gratitude to my supervisor, Mr. Ni Haibin, for his invaluable support throughout my studies. His guidance has greatly facilitated my research journey. I am also deeply thankful to him for providing the funding to support and publish this research

#### REFERENCES

- [1] Taflove, A., & Hagness, S. C. (2021). *Computational Electrodynamics: The Finite-Difference Time-Domain Method* (3rd ed.). Artech House.
- [2] Kuhn, L., Repán, T., & Rockstuhl, C. (2023). Exploiting graph neural networks to perform finite-difference time-domain based optical simulations. *APL Photonics*, 8(3), 1-7. <https://doi.org/10.1063/5.0059455>
- [3] Singh, R., Agarwal, A., & Anthony, B. W. (2020). Design of optical meta-structures with applications to beam engineering using deep learning. *Scientific Reports*, 10(1), 19923.
- [4] Krasikov, S., Tranter, A., Bogdanov, A. and Kivshar, Y., 2022. Intelligent metaphotonics empowered by machine learning. *Opto-Electronic Advances*, 5(3), pp.210147-1.
- [5] Kuhn, L., Repán, T. and Rockstuhl, C., 2023. Exploiting graph neural networks to perform finite-difference time domain based optical simulations. *APL Photonics*, 8(3).
- [6] Ali, M., Haque, A.N., Sadik, N., Ahmed, T. and Baten, M.Z., 2023. Predicting strongly localized resonant modes of light in disordered arrays of dielectric scatterers: a machine learning approach. *Optics Express*, 31(2), pp.826-842.
- [7] Ma, W., Liu, Z., Kudyshev, Z.A., Boltasseva, A., Cai, W. and Liu, Y., 2021. Deep learning for the design of photonic structures. *Nature Photonics*, 15(2), pp.77-90.
- [8] Zhelyeznyakov, M.V., Brunton, S. and Majumdar, A., 2021. Deep learning to accelerate scatterer-to-field mapping for inverse design of dielectric metasurfaces. *ACS Photonics*, 8(2), pp.481-488.
- [9] Kanmaz, T.B., Ozturk, E., Demir, H.V. and Gunduz-Demir, C., 2023. Deep-learning-enabled electromagnetic near-field prediction and inverse design of metasurfaces. *Optica*, 10(10), pp.1373-1382.
- [10] Liu, Z., Zhu, D., Raju, L. and Cai, W., 2021. Tackling photonic inverse design with machine learning. *Advanced Science*, 8(5), p.2002923.
- [11] Singh, R., Agarwal, A. and Anthony, B.W., 2020. Design of optical meta-structures with applications to beam engineering using deep learning. *Scientific Reports*, 10(1), p.19923.
- [12] Li, Y., Wang, Y., Qi, S., Ren, Q., Kang, L., Campbell, S.D., Werner, P.L. and Werner, D.H., 2020. Predicting scattering from complex nano-structures via deep learning. *IEEE Access*, 8, pp.139983-139993.
- [13] Malkiel, I., Nagler, A., Mrejen, M., Arieli, U., Wolf, L. and Suchowski, H., 2017. Deep learning for design and retrieval of nano-photonic structures. *arXiv preprint arXiv:1702.07949*.
- [14] Lumerical Solutions, Inc., 2025; <https://www.lumerical.com/>